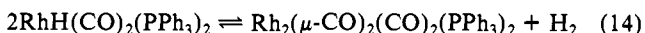


ethylporphyrin) with H<sub>2</sub>, eq 13,<sup>24</sup> and the equilibrium shown as (14) involving the hydroformylation catalyst RhH(CO)<sub>2</sub>(PPh<sub>3</sub>)<sub>2</sub> and a related Rh(0) dimer.<sup>25</sup> Recent studies indicate that the mechanism for (13) proceeds via an odd-electron Rh(II) monomer.<sup>26</sup>



Because of the unusual nature of eq 11, the kinetics and mechanism of the reaction will be investigated further.

### Experimental Section

Benzene was distilled from dark purple solutions of sodium benzo-phenone ketyl under vacuum, and toluene was distilled from CaH<sub>2</sub> under

(24) Wayland, B. B.; Woods, B. A.; Pierce, R. *J. Am. Chem. Soc.* **1982**, *104*, 302.

(25) Evans, D.; Yagupsky, G.; Wilkinson, G. *J. Chem. Soc., Sect. A* **1968**, 2660. Yagupsky, M.; Brown, C. K.; Yagupsky, G.; Wilkinson, G. *J. Chem. Soc., Sect. A* **1970**, 937.

(26) Paonessa, R. S.; Thomas, N. C.; Halpern, J. *J. Am. Chem. Soc.* **1985**, *107*, 4333.

vacuum. The complex [Rh(dppe)<sub>2</sub>](BF<sub>4</sub>) was prepared by literature procedures.<sup>7</sup>

**ESR Measurements.** Samples of Rh(dppe)<sub>2</sub><sup>0</sup> were prepared by reduction of Rh(dppe)<sub>2</sub><sup>+</sup> with sodium naphthalenide in THF as described previously.<sup>7</sup> ESR spectra were recorded at 9.65 GHz on a Bruker ER 200 D spectrometer fitted with a liquid nitrogen flow system and heater/controller for obtaining temperatures down to that of liquid nitrogen.

Spectra were calculated by using a locally modified version of the program EALTW written by Sullivan and Bolton. The local modification incorporates anisotropic broadening as described in the text.

**Reaction of Rh(dppe)<sub>2</sub><sup>0</sup> with H<sub>2</sub>.** A blue solution of Rh(dppe)<sub>2</sub><sup>0</sup> in benzene-d<sub>6</sub> was placed in an NMR tube, which was connected to a vacuum line and sealed under 500 Torr of H<sub>2</sub>. The reaction was followed over a 5-h period by <sup>1</sup>H NMR spectroscopy. The product was identified by comparison with an authentic sample of RhH(dppe)<sub>2</sub> prepared independently by reported procedures.

**Acknowledgment.** We thank the National Science Foundation (CHE 83-08064 and 86-05033) for support of this work and the Johnson Matthey Co., Inc. for a generous loan of rhodium salts. We also acknowledge helpful discussions with Dr. Paul Krusic and Dr. Tom Baker of DuPont and Professor Philip Rieger of Brown University.

## Tetranuclear Iron-Oxo Complexes. Synthesis, Structure, and Properties of Species Containing the Nonplanar {Fe<sub>4</sub>O<sub>2</sub>}<sup>8+</sup> Core and Seven Bridging Carboxylate Ligands

William H. Armstrong, Mary E. Roth, and Stephen J. Lippard\*

Contribution from the Department of Chemistry, Massachusetts Institute of Technology, Cambridge, Massachusetts 02139. Received March 23, 1987

**Abstract:** The synthesis and structure of the novel tetranuclear complexes [Fe<sub>4</sub>O<sub>2</sub>(O<sub>2</sub>CR)<sub>7</sub>(H<sub>2</sub>B(pz)<sub>2</sub>)<sub>2</sub>]<sup>-</sup>, where R = Me or Ph and H<sub>2</sub>B(pz)<sub>2</sub><sup>-</sup> = dihydrobis(1-pyrazolyl)borate, are described. These complexes may be viewed formally as the 2 + 2 condensation products of two {Fe<sub>2</sub>O(O<sub>2</sub>CR)<sub>2</sub>}<sup>2+</sup> cores, containing iron atom pairs Fe<sub>A</sub>Fe<sub>B</sub> and Fe<sub>C</sub>Fe<sub>D</sub>, to form {Fe<sub>4</sub>O<sub>2</sub>(O<sub>2</sub>CR)<sub>4</sub>}<sup>4+</sup>, in which both of the oxo ligands are triply bridging. A four-membered Fe<sub>2</sub>O<sub>2</sub> unit, comprised of iron atoms Fe<sub>B</sub> and Fe<sub>C</sub>, at the center of the tetranuclear complex is bridged by a single benzoate group, and two additional singly bridging benzoate groups link the remaining iron atom pairs, Fe<sub>A</sub>Fe<sub>C</sub> and Fe<sub>B</sub>Fe<sub>D</sub>. In the structure of (Et<sub>4</sub>N)[Fe<sub>4</sub>O<sub>2</sub>(O<sub>2</sub>CPh)<sub>7</sub>(H<sub>2</sub>B(pz)<sub>2</sub>)<sub>2</sub>], the Fe-O (μ<sub>3</sub>-oxo) distances within the {Fe<sub>2</sub>O(O<sub>2</sub>CPh)<sub>2</sub>}<sup>2+</sup> units are 1.822 (7) and 1.854 (8) Å for bonds to Fe<sub>A</sub> and Fe<sub>D</sub> and 1.895 (7) and 1.917 (7) Å for bonds to Fe<sub>B</sub> and Fe<sub>C</sub>. The Fe-O (μ<sub>3</sub>-oxo) bonds linking these halves of the tetranuclear aggregate are 1.955 (8) and 1.967 (8) Å. The {Fe<sub>4</sub>O<sub>2</sub>}<sup>8+</sup> core is distorted from planarity, presumably by the additional bridging carboxylate ligands, with deviations of ±0.5 Å or less from the best plane through the four iron atoms. The deviation of Fe<sub>A</sub> or Fe<sub>D</sub> from the plane defined by the other three iron atoms is 1.8 Å. Proton nuclear magnetic resonance studies of [Fe<sub>4</sub>O<sub>2</sub>(O<sub>2</sub>CR)<sub>7</sub>(H<sub>2</sub>B(pz)<sub>2</sub>)<sub>2</sub>]<sup>-</sup> complexes, dissolved in CD<sub>2</sub>Cl<sub>2</sub>, are consistent with the X-ray structural results. Solution-state magnetic susceptibility data also confirm the integrity of the {Fe<sub>4</sub>O<sub>2</sub>}<sup>8+</sup> core. The optical spectrum of [Fe<sub>4</sub>O<sub>2</sub>(O<sub>2</sub>CR)<sub>7</sub>(H<sub>2</sub>B(pz)<sub>2</sub>)<sub>2</sub>]<sup>-</sup> in solution is similar to, but distinct from, that of the binuclear analogues [Fe<sub>2</sub>O(O<sub>2</sub>CR)<sub>2</sub>(HB(pz)<sub>3</sub>)<sub>2</sub>]. A Raman band at 746 cm<sup>-1</sup> was identified as being characteristic of the {Fe<sub>4</sub>O<sub>2</sub>}<sup>8+</sup> core. Magnetic susceptibility measurements reveal a diamagnetic ground state with antiferromagnetic exchange interactions among the four high-spin ferric centers. Zero-field Mössbauer spectra at four temperatures display a single quadrupole doublet with an isomer shift of 0.52 mm/s, consistent with high-spin Fe(III). The relevance of this chemistry to the synthesis of functional models for the oxo-bridged binuclear iron cores of hemerythrin and related proteins is discussed.

The diiron cores of the marine invertebrate respiratory protein hemerythrin (Hr)<sup>1</sup> and related proteins including ribonucleotide reductase (RR)<sup>2</sup> and the purple acid phosphatases<sup>3</sup> have been the subject of recent modeling studies by bioinorganic chemists.<sup>4-6</sup>

Binuclear iron(III) complexes containing both oxo and carboxylate bridging ligands have been synthesized and shown to be excellent spectroscopic and magnetic models for Hr and RR.<sup>4-6</sup> Reactivity studies of the {Fe<sub>2</sub>O(O<sub>2</sub>CR)<sub>2</sub>}<sup>2+</sup> core have further aided our un-

(1) (a) Wilkins, R. G.; Harrington, P. C. *Adv. Inorg. Biochem.* **1983**, *5*, 51-85. (b) Harrington, P. C.; Wilkins, R. G. *Coord. Chem. Rev.* **1987**, *79*, 195-214.

(2) (a) Sjöberg, B.-M.; Gräslund, A. *Adv. Inorg. Biochem.* **1983**, *5*, 87-110. (b) Lammers, M.; Follman, H. *Struct. Bonding (Berlin)* **1983**, *54*, 27-91.

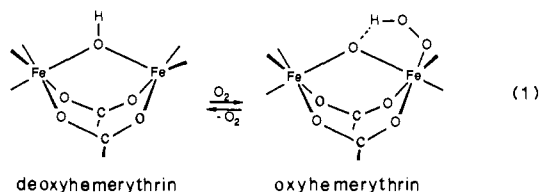
(3) Antanaltis, B. C.; Aisen, P. *Adv. Inorg. Biochem.* **1983**, *5*, 111-136.

(4) (a) Armstrong, W. H.; Lippard, S. J. *J. Am. Chem. Soc.* **1983**, *105*, 4837-4838. (b) Armstrong, W. H.; Spool, A.; Papaefthymiou, G. C.; Frankel, R. B.; Lippard, S. J. *J. Am. Chem. Soc.* **1984**, *106*, 3653-3667.

(5) Wiegardt, K.; Pohl, K.; Gebert, W. *Angew. Chem., Int. Ed. Engl.* **1983**, *22*, 727.

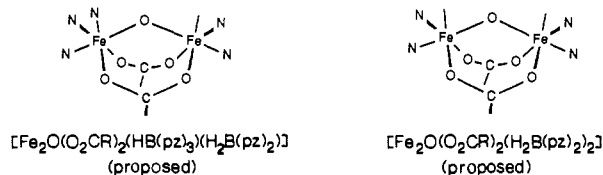
(6) Toftlund, H.; Murray, K. S.; Zwack, P. R.; Taylor, L. F.; Anderson, O. P. *J. Chem. Soc., Chem. Commun.* **1986**, 191-193.

understanding of the chemical properties of Hr.<sup>7,8</sup> In order for these models to mimic the properties of the proteins, however, their diiron cores must be able to undergo reversible oxidation-reduction/deprotonation-protonation cycles without decomposition. The reversible binding of dioxygen in Hr may be written as shown in eq 1.<sup>9</sup> In the semimet forms, a mixed-valence [Fe<sup>II</sup>Fe<sup>III</sup>] species

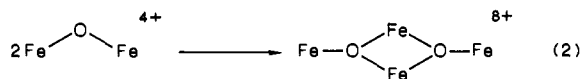


occurs.<sup>1</sup> The hydrotris(1-pyrazolyl)borato-capped model compound previously described by us, [Fe<sub>2</sub>O(O<sub>2</sub>CCH<sub>3</sub>)<sub>2</sub>(HB(pz)<sub>3</sub>)<sub>2</sub>], rapidly decomposes when reduced electrochemically.<sup>4b</sup> The trimethyltriazacyclononane-capped analogue, [Fe<sub>2</sub>O(O<sub>2</sub>CCH<sub>3</sub>)<sub>2</sub>(Me<sub>3</sub>TACN)<sub>2</sub>]<sup>2+</sup>, however, can be reduced quasi-reversibly by electrochemical means to form a [Fe<sup>II</sup>Fe<sup>III</sup>] mixed-valence complex in solution, and a hydroxo-bridged [Fe<sup>II</sup>]<sub>2</sub> derivative has been isolated and structurally characterized.<sup>10</sup>

In addition to the requirement for reversible redox chemistry, functional models of the binuclear iron centers of Hr and RR must also have a vacant coordination site for binding dioxygen, as peroxide or hydroperoxide (see eq 1), as well as other ligands. The synthesis of compounds to achieve this objective was the initial reason for undertaking the studies described here. In particular, we were interested in determining whether use of the dihydrobis(1-pyrazolyl)borate in addition to, or in place of, hydrotris(1-pyrazolyl)borate in chemistry analogous to the synthesis of [Fe<sub>2</sub>O(O<sub>2</sub>CR)<sub>2</sub>(HB(pz)<sub>3</sub>)<sub>2</sub>] would result in a binuclear complex with one or two available coordination sites, as illustrated below:



Although such species have not yet been isolated, the synthetic work produced a very interesting tetranuclear aggregate having the formula [Fe<sub>4</sub>O<sub>2</sub>(O<sub>2</sub>CR)<sub>7</sub>(H<sub>2</sub>B(pz)<sub>2</sub>)<sub>2</sub>]<sup>-</sup>, where R = Ph (1) or Me (2). In parallel work carried out in our laboratory, it was found that a similar tetranuclear iron(III) complex, [Fe<sub>4</sub>O<sub>2</sub>(BICO)<sub>2</sub>(BICOH)<sub>2</sub>] (3), which also contains the {Fe<sub>4</sub>O<sub>2</sub>}<sup>8+</sup> core, is obtained by using the bis(imidazolyl)carbinol ligand (BICOH) in place of H<sub>2</sub>B(pz)<sub>2</sub>.<sup>11</sup> The tendency toward tetranuclear complex formation may result from the residual coordinating ability of the bridging oxo atom in the {Fe<sub>2</sub>O}<sup>4+</sup> core. That is, the tetranuclear species may arise by dimerization of binuclear species as shown in eq 2.



Tetranuclear iron aggregates containing sulfide or carbonyl bridging ligands are well-known.<sup>12</sup> There are relatively few

reports, however, of Fe<sub>4</sub> units having bridging oxo ligands. Recently, a tetranuclear complex with an adamantane-like Fe<sub>4</sub>O<sub>6</sub> core containing oxo, hydroxo, and phenoxo bridging ligands was reported.<sup>13</sup> In addition, a tetranuclear complex consisting of a planar array of iron atoms bridged by oxo, alkoxo, and carbonate ligands has been described.<sup>14</sup> In an attempt to incorporate the {Fe<sub>2</sub>O(O<sub>2</sub>CR)<sub>2</sub>}<sup>2+</sup> core into a binucleating ligand, a tetranuclear compound was isolated in which the hexadentate ligand bridged two weakly interacting {Fe<sub>2</sub>O(O<sub>2</sub>CCH<sub>3</sub>)<sub>2</sub>}<sup>2+</sup> cores.<sup>6</sup> In the above three cases, the oxo atoms are doubly bridging, whereas in 1-3 there are two triply bridging oxo groups. A Russian group has recently reported the synthesis, crystal structure, and Mössbauer spectrum of a complex containing an Fe<sub>4</sub>O<sub>2</sub> unit very similar to those of 1-3, [Fe<sub>4</sub>O<sub>2</sub>(O<sub>2</sub>CCF<sub>3</sub>)<sub>8</sub>(H<sub>2</sub>O)<sub>6</sub>] (4).<sup>15,16</sup> Compounds 1-4 may be considered the next highest members in the series of polynuclear iron-oxo carboxylate complexes, which start with molecules containing the {Fe<sub>2</sub>O(O<sub>2</sub>CR)<sub>2</sub>}<sup>2+</sup>, {Fe<sub>3</sub>O(O<sub>2</sub>CR)<sub>6</sub>}<sup>+</sup>, and {Fe<sub>3</sub>O(O<sub>2</sub>CR)<sub>2</sub>(OR)<sub>2</sub>}<sup>3+</sup> cores.<sup>17</sup> Compounds formulated as [Fe<sub>4</sub>O(O<sub>2</sub>CCH<sub>3</sub>)<sub>10</sub>] and [Fe<sub>2</sub>O(O<sub>2</sub>CCH<sub>3</sub>)<sub>12</sub>](O<sub>2</sub>CCH<sub>3</sub>) have also been reported<sup>18</sup> but have not been characterized by single-crystal X-ray measurements.

In the present paper we report the synthesis, structure, and properties of 1 and 2 and discuss their relationship to other members of the newly emerging class of oxo-bridged polyiron aggregates.

### Experimental Section

**Preparation of Compounds.** Potassium dihydrobis(1-pyrazolyl)borate (KH<sub>2</sub>B(pz)<sub>2</sub>) was purchased from Strem Chemical Inc., Newburyport, MA. (Et<sub>4</sub>N)<sub>2</sub>[Fe<sub>2</sub>OCl<sub>6</sub>] was prepared by a literature procedure.<sup>19</sup> All other reagents and solvents were obtained from commercial sources and used without purification. Elemental analyses were performed by Atlantic Microlab, Inc., Atlanta, GA, and by Galbraith Laboratories, Knoxville, TN.

**Tetraethylammonium Bis(μ<sub>3</sub>-oxo)heptakis(μ-benzoato)bis[dihydrobis(1-pyrazolyl)borato]tetraferate(III), (Et<sub>4</sub>N)<sub>2</sub>[Fe<sub>4</sub>O<sub>2</sub>(O<sub>2</sub>CPh)<sub>7</sub>(H<sub>2</sub>B(pz)<sub>2</sub>)<sub>2</sub>] (1).** To a solution of 1.520 g (2.529 mmol) of (Et<sub>4</sub>N)<sub>2</sub>[Fe<sub>2</sub>OCl<sub>6</sub>] in 75 mL of CH<sub>3</sub>CN was added 1.284 g (8.910 mmol) of solid anhydrous Na(O<sub>2</sub>CC<sub>6</sub>H<sub>5</sub>). The red-brown suspension was stirred vigorously for 1 h. The distinctly different appearance of the precipitate along with a noticeable color change indicated that a reaction had occurred. A solution of 0.473 g (2.54 mmol) of KH<sub>2</sub>B(pz)<sub>2</sub> in 25 mL of MeCN was then added to the stirred suspension, giving rise to a rapid color change to green-brown. After an additional 1 h of stirring, a white solid was filtered from the reaction mixture and washed with MeCN. The MeCN filtrates were combined and concentrated to a thick green-brown oil by using a rotary evaporator. This oil was dissolved in approximately 20-25 mL of CHCl<sub>3</sub>, and the resulting solution was filtered. The filtrate was immediately cooled to -20 °C and stored for several days. The crystalline solid that precipitated during this time was filtered off and dried in the air. In order to remove a colorless impurity, the material was washed three times quickly with small portions of H<sub>2</sub>O and dried first with a stream of air and then under vacuum to afford 1.28 g (66.3% yield) of 1 as a microcrystalline green solid. Further purification was achieved by recrystallization from CH<sub>2</sub>Cl<sub>2</sub>/hexanes by using liquid-liquid diffusion. Two distinctly different crystal forms were observed under these conditions. The proportion of fine needles to large blocks depended on the concentration of the initial CH<sub>2</sub>Cl<sub>2</sub> solution of 1. More concentrated solutions gave a larger amount of the needlelike crystal form. In a typical recrystallization, 0.18-0.27 g of 1 was dissolved in 25 mL of CH<sub>2</sub>Cl<sub>2</sub> and

(7) (a) Armstrong, W. H.; Lippard, S. J. *J. Am. Chem. Soc.* **1984**, *106*, 4632-4633. (b) Armstrong, W. H.; Lippard, S. J. *J. Am. Chem. Soc.* **1985**, *107*, 3730-3731.

(8) Wiegardt, K.; Pohl, K.; Ventur, D. *Angew. Chem., Int. Ed. Engl.* **1985**, *24*, 392-393.

(9) Shiemke, A. K.; Loehr, T. M.; Sanders-Loehr, J. *J. Am. Chem. Soc.* **1986**, *108*, 2437-2443 and references cited therein.

(10) (a) Chaudhuri, P.; Wiegardt, K.; Nuber, B.; Weiss, J. *Angew. Chem., Int. Ed. Engl.* **1985**, *24*, 778-779. (b) Hartman, J.; Rardin, R. L.; Chaudhuri, P.; Weiss, J.; Wiegardt, K.; Lippard, S. J. *J. Am. Chem. Soc.*, in press.

(11) (a) Gorun, S. M. Ph.D. Dissertation, MIT, 1986. (b) Gorun, S. M.; Lippard, S. J. *Inorg. Chem.*, in press. (c) Lippard, S. J. *Chem. Br.* **1986**, *22*, 222-229.

(12) (a) Berg, J. R.; Holm, R. H. *Met. Ions Biol.* **1982**, *4*, 1-66. (b) Chinl, P.; Heaton, B. T. *Top. Curr. Chem.* **1977**, *71*, 1-70.

(13) Murch, B. P.; Boyle, P. D.; Que, L., Jr. *J. Am. Chem. Soc.* **1985**, *107*, 6728-6729.

(14) Jameson, D. L.; Xie, C.-L.; Hendrickson, D. N.; Potenza, J. A.; Schugar, H. J. *J. Am. Chem. Soc.* **1987**, *109*, 740-746.

(15) Ponomarev, V. I.; Atovmyan, L. O.; Bobkova, S. A.; Turtë, K. I. *Dokl. Akad. Nauk SSSR* **1984**, *274*, 368-372.

(16) Stukan, R. A.; Ponomarev, V. I.; Nifontov, V. P.; Turtë, K. I.; Atovmyan, L. O. *J. Struct. Chem.* **1985**, *26*, 197-201.

(17) (a) Cotton, F. A.; Wilkinson, G. *Advanced Inorganic Chemistry*, 4th ed.; Wiley: New York, 1980; pp 154-155. (b) Catterick, J.; Thornton, P. *Adv. Inorg. Chem. Radiochem.* **1977**, *20*, 291-362. (c) Gorun, S. M.; Pappafthymiou, G. C.; Frankel, R. B.; Lippard, S. J. *J. Am. Chem. Soc.* **1987**, *109*, 4244-4255.

(18) Catterick, J.; Thornton, P.; Fitzsimmons, B. W. *J. Chem. Soc., Dalton Trans.* **1977**, 1420-1425.

(19) Armstrong, W. H.; Lippard, S. J. *Inorg. Chem.* **1985**, *24*, 981-982.

~80 mL of hexanes was carefully layered on top in a 100-mL graduated cylinder. Diffusion was allowed to proceed, for up to 10 days in some cases, prior to filtration of the product. When precipitated in this manner, the block-shaped monoclinic form of **1** crystallizes with two CH<sub>2</sub>Cl<sub>2</sub> molecules of solvation. Solvent-free material was prepared by powdering a portion of the crystals, followed by drying at room temperature under vacuum for ~12 h. Anal. Calcd for C<sub>69</sub>H<sub>71</sub>B<sub>2</sub>Fe<sub>4</sub>N<sub>9</sub>O<sub>16</sub>: C, 54.26; H, 4.69; N, 8.25. Found: C, 54.06; H, 4.75; N, 8.17. <sup>1</sup>H NMR (CD<sub>2</sub>Cl<sub>2</sub>, 295 K, 250 MHz): δ 17.1, 13.5, 12.5 (8 pyrazole H<sub>4</sub> and H<sub>5</sub> protons); 9.3, 8.0 (v br), 7.3, 6.5, 6.0 (phenyl protons and H<sub>3</sub> pyrazole); 1.9 (12 hydroborate and CH<sub>2</sub> protons); 0.6 (12 CH<sub>3</sub> protons). UV-vis/near-IR (CH<sub>2</sub>Cl<sub>2</sub>, 5 × 10<sup>-4</sup> M): λ, nm (ε<sub>Fe</sub>, cm<sup>-1</sup> M<sup>-1</sup>) 265 (sh), 300 (sh), 350 (3300), 467 (470), 565 (sh, 75) 1020 (8). FTIR (KBr, cm<sup>-1</sup>): 2406, 2286, 1602, 1563, 1545, 1400 (vs), 1298, 1215, 1176, 1154, 1065 (sh), 1058, 1026, 1000, 985, 884, 761, 720, 687, 674, 661, 639, 524, 469.

**Tetraethylammonium Bis(μ<sub>3</sub>-oxo)heptakis(μ-acetato)bis(dihydrobis(1-pyrazolylborato))tetraferate(III) (2).** In a manner analogous to that described for **1**, 1.519 g (2.529 mmol) of (Et<sub>4</sub>N)<sub>2</sub>[Fe<sub>2</sub>OCl<sub>6</sub>] in 150 mL of CH<sub>3</sub>CN was allowed to react with 0.727 g (8.866 mmol) of NaO<sub>2</sub>C-CH<sub>3</sub> for 3 h. To the vigorously stirring solution, 0.472 g (2.54 mmol) of KH<sub>2</sub>B(pz)<sub>2</sub> in 50 mL of CH<sub>3</sub>CN was added over several minutes. The cloudy, green-brown solution was stirred for another 2 h and stored at -20 °C overnight. Suction filtration was used to remove an off-white solid. The solvent was removed from the filtrate under vacuum and the residue dissolved in ~25 mL of CHCl<sub>3</sub>. The crystalline material, which was collected after 3 days, was contaminated with a white solid. This solid was removed by washing with small amounts of water. The remaining green powder was dried under vacuum to yield 0.932 g (67.5%) of **2**. The compound was recrystallized by dissolving it in CH<sub>3</sub>CN, concentrating to an oil, taking up the residue in CHCl<sub>3</sub>, and letting the solution stand at -20 °C. After 24 h, the product was collected as a dark green microcrystalline solid, which appears to lose solvent on drying. This material was powdered and dried under vacuum for 24 h at room temperature to remove any residual solvent. Anal. Calcd for C<sub>34</sub>H<sub>57</sub>B<sub>2</sub>Fe<sub>4</sub>N<sub>9</sub>O<sub>16</sub>: C, 37.4; H, 5.26; N, 11.53. Found: C, 36.5; H, 5.22; N, 11.32. <sup>1</sup>H NMR (CD<sub>2</sub>Cl<sub>2</sub>, 250 MHz): δ 17.3, 16.9 (sh), 14.1 (sh), 13.4, 12.5, 10.9 (v br), 8.0 (v br), 3.09, 1.27. FTIR (KBr, cm<sup>-1</sup>): 2407, 2287, 1737, 1590 (s), 1562, 1420 (s), 1343, 1299, 1209, 1199, 1186, 1155, 1058, 1024, 1000, 984, 885, 763, 684, 661, 648, 617, 558, 497. UV-vis/near-IR (CH<sub>2</sub>Cl<sub>2</sub>): λ, nm (ε<sub>Fe</sub>, cm<sup>-1</sup> M<sup>-1</sup>) 255 (sh), 317 (2400), 350 (2700), 466 (440), 570 (60), 1020 (~5).

**Collection and Reduction of X-ray Data.** Block-shaped crystals of **1**, grown from CH<sub>2</sub>Cl<sub>2</sub>/hexanes as described above, appear deep green (almost black) by reflected light and red by transmitted light. One such crystal of dimensions 0.15 × 0.20 × 0.28 mm was chosen for the X-ray experiments and flame-sealed into a glass capillary to prevent loss of solvent from the crystal lattice. On the basis of ω scans of several low-angle reflections, the crystal quality was judged to be acceptable (Δω<sub>1/2</sub> ~ 0.3°). The orientation matrix and unit cell parameters were determined from the setting angles of 25 reflections with 20.1° ≤ 2θ ≤ 32.4°. Intensities of three standard reflections, monitored every 1 h, were constant throughout the data collection. Owing to the rather small variations observed in the azimuthal scans of several reflections well distributed in reciprocal space, no absorption correction was applied to the data.

The diffractometer data showed the crystal to belong to the monoclinic crystal system with systematic absences 0k0, k = 2n + 1, consistent with either space group P2<sub>1</sub> (C<sub>2</sub><sup>h</sup>, No. 4)<sup>20</sup> or P2<sub>1</sub>/m (C<sub>2</sub><sup>h</sup>, No. 11).<sup>20</sup> Statistical tests supported the choice of the noncentric space group. Moreover, in the higher symmetry space group, barring disorder, the anion would have C<sub>i</sub> or C<sub>s</sub> point symmetry, which is incompatible with its structure (see below). Further details of the data collection and reduction are given in ref 21 and Table I.

**Structure Solution and Refinement.** Assuming the noncentric space group choice P2<sub>1</sub>, the direct-methods program MULTAN yielded trial positions for the four iron atoms. Positions of all remaining non-hydrogen atoms, with the exception of the carbon atom of the disordered CH<sub>2</sub>Cl<sub>2</sub> molecule (see below), were obtained from subsequent difference Fourier maps. Two CH<sub>2</sub>Cl<sub>2</sub> molecules of solvation were located in the asymmetric unit. The first, with atom labels C70, Cl1, and Cl2, was ordered and refined with anisotropic thermal parameters. The second solvent molecule was disordered between two distinct positions, with Cl3 and Cl6 defining one molecular orientation and Cl4 and Cl5 the other. The intramolecular nonbonded Cl...Cl distances for the disordered CH<sub>2</sub>Cl<sub>2</sub>

**Table I.** Summary of Crystal Data, Intensity Collection, and Structure Refinement Parameters for (Et<sub>4</sub>N)[Fe<sub>4</sub>O<sub>2</sub>(O<sub>2</sub>CPh)<sub>7</sub>(H<sub>2</sub>B(pz)<sub>2</sub>)<sub>2</sub>]·2CH<sub>2</sub>Cl<sub>2</sub><sup>a</sup>

formula	C <sub>71</sub> H <sub>73</sub> B <sub>2</sub> Cl <sub>4</sub> Fe <sub>4</sub> N <sub>9</sub> O <sub>16</sub>
formula wt	1697.3
space group	P2 <sub>1</sub>
a, Å	13.846 (1)
b, Å	22.663 (5)
c, Å	14.025 (2)
β, deg	115.26 (1)
V, Å <sup>3</sup>	3980.1
Z	2
D <sub>calcd</sub> , g cm <sup>-3</sup>	1.416
D <sub>obsd</sub> , <sup>b</sup> g cm <sup>-3</sup>	1.42 (1)
radiation	Mo Kα (0.71073 Å)
abs coeff, cm <sup>-1</sup>	9.13
data collected	3° ≤ 2θ ≤ 51°; ±h, ±k, ±l
total no. of data collected	7939
average, R <sub>av</sub>	0.022
total no. of unique data	7596
no. of unique data with I > 2σ(I)	3936
no. of variable param	601
R <sub>1</sub> <sup>c</sup>	0.060
R <sub>2</sub>	0.061

<sup>a</sup> All measurements were at room temperature. <sup>b</sup> By suspension in a mixture of CCl<sub>4</sub> and hexane. <sup>c</sup> R<sub>1</sub> = Σ||F<sub>o</sub>| - |F<sub>c</sub>||/Σ|F<sub>o</sub>|; R<sub>2</sub> = [Σw(|F<sub>o</sub>|<sup>2</sup> - |F<sub>c</sub>|<sup>2</sup>)/Σw|F<sub>o</sub>|<sup>2</sup>]<sup>1/2</sup>.

molecules (2.62, 2.58 Å) are somewhat shorter than the corresponding value for the well-ordered solvent (2.89 Å), at least partially due to the fact that neither carbon atom for the disordered solvate was located on the final difference Fourier map. The four Cl atom positions of the disordered CH<sub>2</sub>Cl<sub>2</sub> molecules were refined with isotropic thermal parameters, and their occupancies were both fixed at 0.5. All Fe and O atoms were refined by using anisotropic thermal parameters, as were the non-hydrogen atoms of the H<sub>2</sub>B(pz)<sub>2</sub><sup>-</sup> ligands and the Et<sub>4</sub>N<sup>+</sup> counterion. Phenyl rings were treated as rigid groups with individual isotropic thermal parameters assigned to each atom. Toward the end of the refinement, all hydrogen atoms except those attached to B1, B2, C64, and C65 and the H atoms of the CH<sub>2</sub>Cl<sub>2</sub> molecules were placed at calculated positions, d(C-H) = 0.95 Å, and constrained to "ride" on the carbon atoms to which they were attached. Their positions were fixed during the final refinement cycles. Common isotropic thermal parameters were used for each of the following atom groups: (1) phenyl ring H atoms, (2) pyrazolyl ring H atoms, (3) methylene group H atoms, and (4) methyl group H atoms. After convergence of the structure refinement using the original choice of hand, the discrepancy indices were R<sub>1</sub> = 0.061 and R<sub>2</sub> = 0.063. Refinement was then carried out with the opposite hand, resulting in marginally lower R values (Table I). The latter result is the one reported here. The function minimized during refinement was Σw(|F<sub>o</sub>| - |F<sub>c</sub>|)<sup>2</sup>, where w = 1.1020/[σ<sup>2</sup>(F<sub>o</sub>) + 0.000625(F<sub>o</sub>)<sup>2</sup>]. The largest ratio of parameter shift to estimated standard deviation in the final cycle of refinement was 0.04, with most being ≤ 0.01, and the largest peak in the final difference Fourier map was 1.0 e Å<sup>-3</sup>. Final non-hydrogen atomic positional parameters are given in Table II, and a list of interatomic distances and angles is given in Table III. A listing of observed and calculated structure factors is supplied in Table S1, and the final thermal parameters for non-hydrogen atoms are given in Table S2. Hydrogen atom parameters are listed in Table S3, and geometric parameters for the ligands, cation, and solvent are supplied in Table S4 (Tables S1-S4 in supplementary material).

**Other Physical Measurements.** UV-vis/near-IR spectral measurements were made with use of a Perkin-Elmer Lambda 9 spectrophotometer. The <sup>1</sup>H NMR spectra were recorded with a Bruker WM-250 instrument containing CH<sub>2</sub>Cl<sub>2</sub> as an internal reference (δ 5.32). Positive shifts are referred to, and reported as downfield from, tetramethylsilane. FTIR spectra were recorded with an IBM System 9000 interfaced to an IBM IR/32 spectrometer. Pellets for the IR spectra were prepared from 0.2 mg of **1** or 1 mg of **2** mixed with 100 mg of KBr. Solution magnetic susceptibilities of **1** and **2** were measured in CD<sub>2</sub>Cl<sub>2</sub> by using the Evans method.<sup>22a,b</sup> Diamagnetic corrections of -781 × 10<sup>-6</sup> cgs mol<sup>-1</sup> for **1** and

(20) *International Tables for X-ray Crystallography*, 3rd ed.; Kynoch: Birmingham, England, 1969; Vol. I, pp 79 and 93.

(21) Silverman, L. D.; Dewan, J. C.; Glandomenico, C. M.; Lipppard, S. *J. Inorg. Chem.* **1980**, *19*, 3379-3383.

(22) (a) Evans, D. F. *J. Chem. Soc.* **1958**, 2003-2005. (b) Live, D. H.; Chan, S. I. *Anal. Chem.* **1970**, *42*, 791-792. (c) Mulay, L. N. In *Physical Methods of Chemistry. Part IV. Determination of Mass, Transport, and Electrical-Magnetic Properties*; Welsberger, A., Rossiter, B. W., Eds.; Wiley: New York, 1972; Chapter VIII. (d) Earnshaw, A. *Introduction to Magnetochemistry*; Academic: London, 1968. (e) Weast, R. C., Ed. *Handbook of Chemistry and Physics*; CRC: Boca Raton, FL, 1983; p E-115.

Table II. Final Positional Parameters for Non-Hydrogen Atoms of  $(\text{Et}_4\text{N})[\text{Fe}_4\text{O}_2(\text{O}_2\text{CPh})_7(\text{H}_2\text{B}(\text{pz})_2)_2] \cdot 2\text{CH}_2\text{Cl}_2^{a,b}$ 

atom	X	Y	Z	atom	X	Y	Z
Fe1	-0.20782 (14)	-0.14864 (11)	-0.33320 (14)	C37	-0.3687 (8)	0.0090 (3)	-0.4992 (8)
Fe2	-0.25674 (14)	-0.26986 (11)	-0.37404 (14)	C38	-0.4480 (8)	0.0276 (3)	-0.5956 (8)
Fe3	-0.02156 (14)	-0.25000	-0.16887 (13)	C39	-0.4827 (8)	0.0861 (3)	-0.6086 (8)
Fe4	-0.33906 (14)	-0.17430 (11)	-0.59048 (13)	C40	-0.4382 (8)	0.1259 (3)	-0.5252 (8)
O1	-0.1526 (6)	-0.2243 (4)	-0.2622 (6)	C41	-0.3590 (8)	0.1072 (3)	-0.4287 (8)
O2	-0.2963 (6)	-0.1951 (4)	-0.4505 (6)	C42	-0.3242 (8)	0.0487 (3)	-0.4158 (8)
O3	-0.3232 (6)	-0.1549 (4)	-0.2767 (6)	O15	-0.1852 (6)	-0.1612 (4)	-0.5711 (5)
O4	-0.3687 (6)	-0.2502 (4)	-0.3187 (6)	O16	-0.1008 (6)	-0.1369 (4)	-0.4005 (6)
C1	-0.3805 (10)	-0.1986 (6)	-0.2865 (9)	C43	-0.1060 (10)	-0.1451 (6)	-0.4905 (10)
C2	-0.4715 (6)	-0.1928 (4)	-0.2580 (6)	C44	-0.0057 (6)	-0.1328 (4)	-0.5037 (7)
C3	-0.5271 (6)	-0.2426 (4)	-0.2503 (6)	C45	0.0803 (6)	-0.1055 (4)	-0.4221 (7)
C4	-0.6139 (6)	-0.2364 (4)	-0.2253 (6)	C46	0.1720 (6)	-0.0913 (4)	-0.4350 (7)
C5	-0.6451 (6)	-0.1804 (4)	-0.2080 (6)	C47	0.1778 (6)	-0.1045 (4)	-0.5297 (7)
C6	-0.5895 (6)	-0.1306 (4)	-0.2158 (6)	C48	0.0918 (6)	-0.1317 (4)	-0.6113 (7)
C7	-0.5027 (6)	-0.1368 (4)	-0.2408 (6)	C49	0.0001 (6)	-0.1459 (4)	-0.5983 (7)
O5	-0.0969 (7)	-0.1056 (4)	-0.2102 (6)	B1	0.0996 (17)	-0.3036 (8)	0.0921 (14)
O6	0.0452 (6)	-0.1672 (4)	-0.1554 (6)	B2	-0.5709 (16)	-0.1228 (9)	-0.8057 (15)
C8	0.0055 (11)	-0.1175 (7)	-0.1736 (10)	N1	0.1368 (7)	-0.2747 (5)	-0.0638 (8)
C9	0.0766 (8)	-0.0669 (4)	-0.1555 (8)	N2	0.1744 (9)	-0.2910 (5)	0.0379 (8)
C10	0.1870 (8)	-0.0747 (4)	-0.1044 (8)	C50	0.2835 (12)	-0.2937 (8)	0.0831 (12)
C11	0.2551 (8)	-0.0273 (4)	-0.0939 (8)	C51	0.3144 (12)	-0.2802 (9)	0.0064 (13)
C12	0.2129 (8)	0.0279 (4)	-0.1344 (8)	C52	0.2209 (11)	-0.2688 (7)	-0.0832 (12)
C13	0.1025 (8)	0.0357 (4)	-0.1855 (8)	N3	-0.0468 (8)	-0.2328 (5)	-0.0330 (7)
C14	0.0344 (8)	-0.0117 (4)	-0.1960 (8)	N4	0.0183 (8)	-0.2519 (5)	0.0670 (8)
O7	-0.0642 (7)	-0.3378 (4)	-0.1720 (6)	C53	-0.0070 (14)	-0.2219 (7)	0.1349 (11)
O8	-0.2335 (7)	-0.3460 (4)	-0.2925 (7)	C54	-0.0869 (13)	-0.1838 (9)	0.0810 (12)
C15	-0.1479 (11)	-0.3648 (6)	-0.2211 (10)	C55	-0.1103 (11)	-0.1916 (6)	-0.0253 (11)
C16	-0.1479 (8)	-0.4286 (3)	-0.1942 (8)	N5	-0.3768 (9)	-0.1604 (6)	-0.7524 (8)
C17	-0.0630 (8)	-0.4512 (3)	-0.1055 (8)	N6	-0.4773 (11)	-0.1476 (6)	-0.8276 (8)
C18	-0.0595 (8)	-0.5112 (3)	-0.0821 (8)	C56	-0.4799 (15)	-0.1570 (8)	-0.9209 (12)
C19	-0.1410 (8)	-0.5486 (3)	-0.1474 (8)	C57	-0.3809 (17)	-0.1736 (11)	-0.9106 (13)
C20	-0.2259 (8)	-0.5259 (3)	-0.2361 (8)	C58	-0.3234 (13)	-0.1781 (10)	-0.8036 (13)
C21	-0.2293 (8)	-0.4659 (3)	-0.2596 (8)	N7	-0.5044 (8)	-0.1796 (5)	-0.6320 (8)
O9	0.0219 (6)	-0.2690 (4)	-0.2894 (6)	N8	-0.5846 (9)	-0.1640 (5)	-0.7257 (8)
O10	-0.1390 (6)	-0.2921 (4)	-0.4212 (6)	C59	-0.6765 (11)	-0.1873 (8)	-0.7302 (13)
C22	-0.0393 (11)	-0.2817 (6)	-0.3824 (10)	C60	-0.6589 (12)	-0.2127 (7)	-0.6388 (16)
C23	0.0087 (7)	-0.2868 (4)	-0.4599 (6)	C61	-0.5499 (13)	-0.2102 (7)	-0.5781 (11)
C24	0.1177 (7)	-0.2763 (4)	-0.4252 (6)	N9	0.1446 (13)	-0.4626 (6)	-0.3173 (12)
C25	0.1656 (7)	-0.2842 (4)	-0.4940 (6)	C62	0.031 (2)	-0.4824 (9)	-0.3462 (16)
C26	0.1044 (7)	-0.3025 (4)	-0.5974 (6)	C63	-0.0592 (16)	-0.4371 (9)	-0.4009 (17)
C27	-0.0047 (7)	-0.3129 (4)	-0.6321 (6)	C64	0.2096 (18)	-0.5210 (10)	-0.265 (2)
C28	-0.0525 (7)	-0.3051 (4)	-0.5634 (6)	C65	0.328 (3)	-0.5036 (11)	-0.221 (2)
O11	-0.3545 (6)	-0.3143 (4)	-0.5026 (7)	C66	0.1459 (14)	-0.4405 (9)	-0.4212 (16)
O12	-0.3423 (6)	-0.2622 (4)	-0.6332 (6)	C67	0.1093 (19)	-0.4769 (10)	-0.5101 (18)
C29	-0.3598 (11)	-0.3087 (7)	-0.5946 (11)	C68	0.173 (2)	-0.4112 (10)	-0.2419 (16)
C30	-0.3941 (8)	-0.3611 (4)	-0.6644 (8)	C69	0.181 (2)	-0.4210 (14)	-0.135 (3)
C31	-0.4239 (8)	-0.3561 (4)	-0.7724 (8)	C70	-0.2601 (15)	-0.0255 (9)	-0.1526 (15)
C32	-0.4597 (8)	-0.4057 (4)	-0.8372 (8)	C11	-0.2820 (5)	-0.0561 (3)	-0.0467 (4)
C33	-0.4657 (8)	-0.4602 (4)	-0.7939 (8)	C12	-0.2118 (5)	0.0459 (3)	-0.1244 (4)
C34	-0.4360 (8)	-0.4652 (4)	-0.6858 (8)	C13	-0.4311 (13)	-0.3879 (7)	-0.0995 (11)
C35	-0.4002 (8)	-0.4157 (4)	-0.6211 (8)	C14	-0.2604 (12)	-0.3120 (7)	0.0586 (13)
O13	-0.3483 (6)	-0.0846 (4)	-0.5646 (6)	C15	-0.3463 (15)	-0.3810 (8)	-0.1019 (14)
O14	-0.2754 (7)	-0.0694 (4)	-0.3905 (6)	C16	-0.2518 (19)	-0.3279 (11)	-0.019 (2)
C36	-0.3288 (10)	-0.0540 (6)	-0.4821 (11)				

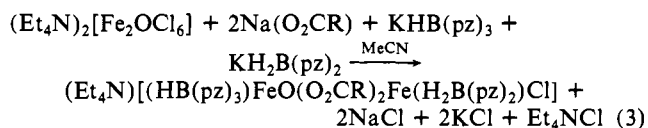
<sup>a</sup> Atoms are labeled as shown in Figure 1a. <sup>b</sup> Estimated standard deviations, in parentheses, occur in the last significant figure(s) for each parameter.

$-522 \times 10^{-6}$  cgs mol<sup>-1</sup> for **2** were calculated from Pascal's constants.<sup>22c</sup> A constitutive correction of  $+8.0 \times 10^{-6}$  cgs mol<sup>-1</sup> was applied for each pyrazole ring, and the following values were used for other groups: benzoate,  $-67.12 \times 10^{-6}$  cgs mol<sup>-1</sup>; acetate,  $-30 \times 10^{-6}$  cgs mol<sup>-1</sup>; O<sup>2-</sup>,  $-7 \times 10^{-6}$  cgs mol<sup>-1</sup>.<sup>22d</sup> The mass susceptibility of CD<sub>2</sub>Cl<sub>2</sub> was taken to be  $-0.549 \times 10^{-6}$  cgs g<sup>-1</sup>.<sup>22e</sup> Solid-state magnetic measurements were carried out with an SHE Model 905 SQUID-type susceptometer operating at 20 kG in the range 6–300 K. A 19.99-mg analytically pure sample of **1** in a calibrated Al–Si container with a Kel-F lid was used for the data collection. A Spex 1401 double monochromator equipped with a cooled RCA 31034 photomultiplier tube with photon-counting electronics was used to acquire the Raman spectra. The spectrometer was interfaced with a North Star computer for ease of collection, manipulation, storage, and plotting of data. The spectra were recorded on a 4662 Tektronix Interactive Digital Plotter. A tunable argon laser (Coherent Radiation Model 52 and Spectra Physics Model 164) was used. The data in Figure 6 were obtained for a 95 mM solution (MeCN) of **1** contained in a spinning 5-mm NMR tube using a back-scattering geometry. The power incident at the sample was 40–50 mW, and the slits were set at 200/250/200 μm. The Mössbauer spectra were recorded by using a

conventional constant-acceleration spectrometer equipped with a temperature controller, maintaining temperatures within  $\pm 0.1$  K. The  $\gamma$ -ray source was <sup>57</sup>Co in Rh metal.

## Results and Discussion

**Synthesis.** Equation 3 displays the reaction stoichiometry initially anticipated, the intent being to prepare the asymmetrically capped  $[\text{Fe}_2\text{O}(\text{O}_2\text{CR})_2(\text{HB}(\text{pz})_3)(\text{H}_2\text{B}(\text{pz})_2)]$  analogue (vide supra) of the Hr model complex  $[\text{Fe}_2\text{O}(\text{O}_2\text{CR})_2(\text{HB}(\text{pz})_3)_2]$ . The



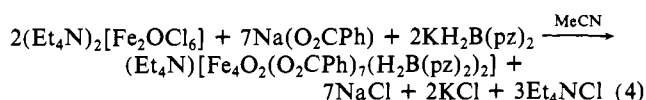
likelihood of obtaining a mixture of products was recognized; however, it was anticipated that, by using fractional crystallization techniques, one might be able to isolate the desired compound.

**Table III.** Selected Interatomic Distances (Å) and Angles (deg) for the Anion in  $(\text{Et}_4\text{N})[\text{Fe}_4\text{O}_2(\text{O}_2\text{CPh})_7(\text{H}_2\text{B}(\text{pz})_2)_2]^-$ <sup>a</sup>

Fe1...Fe2	2.829 (4)	Fe1-O1	1.967 (8)
Fe1...Fe3	3.488 (2)	Fe1-O2	1.895 (7)
Fe1...Fe4	3.326 (2)	Fe1-O3	2.070 (10)
Fe2...Fe3	3.330 (2)	Fe1-O5	2.006 (7)
Fe2...Fe4	3.500 (3)	Fe1-O14	2.027 (9)
Fe3...Fe4	5.920 (2)	Fe1-O16	2.085 (10)
Fe2-O1	1.917 (7)	Fe3-N1	2.129 (9)
Fe2-O2	1.955 (8)	Fe3-N3	2.115 (12)
Fe2-O4	2.057 (10)	Fe3-O1	1.822 (7)
Fe2-O8	2.019 (9)	Fe3-O6	2.065 (9)
Fe2-O10	2.067 (10)	Fe3-O7	2.070 (9)
Fe2-O11	2.003 (8)	Fe3-O9	2.068 (10)
Fe4-N5	2.125 (12)	O1-Fe1-O2	85.6 (3)
Fe4-N7	2.111 (11)	O1-Fe1-O3	86.8 (4)
Fe4-O2	1.854 (8)	O1-Fe1-O5	89.9 (3)
Fe4-O12	2.075 (10)	O1-Fe1-O14	171.0 (4)
Fe4-O13	2.079 (9)	O1-Fe1-O16	98.2 (4)
Fe4-O15	2.051 (9)	O2-Fe1-O3	88.6 (4)
Fe2...Fe1...Fe3	62.61 (6)	Fe1...Fe2...Fe3	68.43 (5)
Fe2...Fe1...Fe4	68.77 (7)	Fe1...Fe2...Fe4	62.35 (7)
Fe3...Fe1...Fe4	120.61 (9)	Fe3...Fe2...Fe4	120.15 (8)
Fe1...Fe3...Fe2	48.96 (6)	Fe1...Fe4...Fe2	48.88 (6)
Fe1...Fe3...Fe4	28.92 (4)	Fe1...Fe4...Fe3	30.47 (5)
Fe2...Fe3...Fe4	30.75 (5)	Fe2...Fe4...Fe3	29.10 (4)
O1-Fe2-O2	85.4 (3)	O2-Fe1-O5	171.9 (4)
O1-Fe2-O4	89.9 (4)	O2-Fe1-O14	97.5 (3)
O1-Fe2-O8	96.5 (3)	O2-Fe1-O16	89.9 (4)
O1-Fe2-O10	88.5 (4)	O3-Fe1-O5	97.8 (4)
O1-Fe2-O11	172.1 (4)	O3-Fe1-O14	84.9 (4)
O2-Fe2-O4	86.5 (4)	O3-Fe1-O16	174.7 (3)
O2-Fe2-O8	172.5 (4)	O5-Fe1-O14	88.0 (3)
O2-Fe2-O10	96.4 (4)	O5-Fe1-O16	84.0 (4)
O2-Fe2-O11	91.0 (3)	O14-Fe1-O16	90.3 (4)
O4-Fe2-O8	86.3 (4)	N1-Fe3-N3	86.7 (4)
O4-Fe2-O10	176.6 (3)	N1-Fe3-O1	175.6 (4)
O4-Fe2-O11	96.9 (4)	N1-Fe3-O6	83.5 (4)
O8-Fe2-O10	90.9 (4)	N1-Fe3-O7	87.8 (4)
O8-Fe2-O11	87.9 (3)	N1-Fe3-O9	86.4 (4)
O10-Fe2-O11	84.9 (4)	N3-Fe3-O1	95.2 (4)
N5-Fe4-N7	88.3 (5)	N3-Fe3-O6	89.4 (4)
N5-Fe4-O2	172.5 (5)	N3-Fe3-O7	92.4 (4)
N5-Fe4-O12	82.4 (4)	N3-Fe3-O9	173.1 (3)
N5-Fe4-O13	92.1 (4)	O1-Fe3-O6	92.6 (3)
N5-Fe4-O15	83.6 (4)	O1-Fe3-O7	96.0 (3)
N7-Fe4-O2	95.5 (4)	O1-Fe3-O9	91.6 (4)
N7-Fe4-O12	88.8 (4)	O6-Fe3-O7	171.0 (3)
N7-Fe4-O13	87.9 (4)	O6-Fe3-O9	89.3 (4)
N7-Fe4-O15	171.0 (4)	O7-Fe3-O9	87.8 (4)
O2-Fe4-O12	91.1 (4)	Fe1-O1-Fe2	93.5 (3)
O2-Fe4-O13	94.6 (4)	Fe1-O1-Fe3	134.1 (5)
O2-Fe4-O15	93.0 (3)	Fe2-O1-Fe3	125.9 (5)
O12-Fe4-O13	173.7 (3)	Fe1-O2-Fe2	94.5 (3)
O12-Fe4-O15	94.0 (4)	Fe1-O2-Fe4	125.1 (5)
O13-Fe4-O15	88.5 (4)	Fe2-O2-Fe4	133.6 (5)

<sup>a</sup>See Figure 1 for atom-labeling scheme.

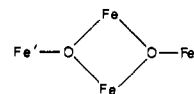
When R = Ph in eq 3, two products were isolated from the reaction mixture, neither one of which was the desired asymmetric species. The first product was easily identified as  $[\text{Fe}_2\text{O}(\text{O}_2\text{CPh})_2(\text{HB}(\text{pz})_2)_2]$  by its UV-vis spectrum.<sup>4b</sup> The second product was the tetranuclear aggregate,  $(\text{Et}_4\text{N})[\text{Fe}_4\text{O}_2(\text{O}_2\text{CPh})_7(\text{H}_2\text{B}(\text{pz})_2)_2]^-$  (**1**), the identity of which was established in a single-crystal X-ray structure determination (see below). Once the composition of the tetranuclear aggregate was revealed by crystallography, its synthesis was optimized by use of the reaction sequence given in eq 4. During this reaction, alkali chloride salts precipitate and are



easily separated by filtration. Removal of MeCN from the filtrate and crystallization of the resulting oil from  $\text{CHCl}_3$  at  $-20^\circ\text{C}$  gave

**Table IV.** Comparison of Selected Structural Parameters of the  $\text{Fe}_4\text{O}_2$  Cores of  $(\text{Et}_4\text{N})[\text{Fe}_4\text{O}_2(\text{O}_2\text{CPh})_7(\text{H}_2\text{B}(\text{pz})_2)_2] \cdot 2\text{CH}_2\text{Cl}_2$  (**1**) and  $[\text{Fe}_4\text{O}_2(\text{O}_2\text{CCF}_3)_8(\text{H}_2\text{O})_6] \cdot 2\text{H}_2\text{O}$  (**4**)

	<b>1</b>	<b>4</b>
Fe...Fe <sup>a</sup>	2.829 (4)	2.915 (3)
Fe...Fe'	3.326 (2), 3.330 (2); 3.488 (2), 3.500 (3)	3.476 (2), 3.436 (3)
Fe'...Fe'	5.920 (2)	6.276 (4)
Fe-O	1.895 (7), 1.917 (7); 1.955 (8), 1.967 (8)	1.936 (3), 1.961 (3)
Fe'-O	1.822 (7), 1.854 (8)	1.842 (4)
Fe-O-Fe	93.5 (3), 94.5 (3)	96.5 (2)
Fe'-O-Fe	125.1 (5), 125.9 (5); 133.6 (5), 134.1 (5)	133.9 (2), 129.5 (2)
O-Fe-O	85.4 (3), 85.6 (3)	82.9 (2)

<sup>a</sup>Labels Fe and Fe' refer to the diagram below:See also Figure 3 for a diagram of the  $[\text{Fe}_4\text{O}_2]^{8+}$  core in **1**.

a mixture of microcrystalline **1** contaminated with a white solid, presumed to be  $\text{Et}_4\text{NCl}$ . The latter material could be washed away with small portions of water without leading to significant decomposition of the desired products. The major species formed is the tetranuclear aggregate, **1**, isolated from the reaction mixture in reasonably good yield (66%). UV-visible spectroscopy (see below), used to follow the reaction, revealed fairly clean formation of **1**, in  $\sim 80\%$  yield. The acetate analogue **2** was prepared when  $\text{Na}(\text{O}_2\text{CCH}_3)$  was substituted for  $\text{Na}(\text{O}_2\text{CPh})$  in eq 4.

The identity of the soluble ferric carboxylate species that exists in MeCN solution prior to the addition of dihydrobis(1-pyrazolyl)borate in this study, or of hydrotris(1-pyrazolyl)borate, as reported previously, has not been established.<sup>4</sup> Recently, however, an undecanuclear ferric carboxylate species was isolated from a similar MeCN/aqueous THF reaction mixture, prior to the addition of any nitrogen-containing ligands.<sup>11,23</sup> The synthetic method used to obtain  $[\text{Fe}_4\text{O}_2(\text{O}_2\text{CCF}_3)_8(\text{H}_2\text{O})_6] \cdot 2\text{H}_2\text{O}$  (**4**) was described only briefly.<sup>15,16</sup> In one case,<sup>15</sup> this product was crystallized from a solution of the mixed-valence trinuclear complex,  $[\text{Fe}_3\text{O}(\text{O}_2\text{CCF}_3)_6(\text{H}_2\text{O})_3] \cdot 3.5\text{H}_2\text{O}$ , while in another report,<sup>16</sup> **4** was prepared "by the interaction of the crystalline trinuclear ferric acetate complex or basic iron acetate with excess solution of trifluoroacetic acid". These results indicate that the classical trinuclear ( $\mu_3$ -oxo)triiron(III) structure can be converted to novel tetranuclear species under the appropriate conditions. In the present case, one might envision formation of the tetranuclear core as occurring through dimerization of binuclear complexes, although the mechanism of formation is not necessarily related to this formal conception.

Aggregation of oxo-bridged bi- and trinuclear iron complexes to form higher clusters appears to be a general phenomenon that should lead to additional discrete molecules or ions other than the  $\text{Fe}_4$ ,<sup>11,13-16</sup>  $\text{Fe}_8$ ,<sup>8</sup> and  $\text{Fe}_{11}$ ,<sup>23</sup> species reported thus far.

**Description of the Structure.** The crystal structure is built from an asymmetric unit comprised of anion **1**, a  $\text{Et}_4\text{N}^+$  cation, and two  $\text{CH}_2\text{Cl}_2$  molecules of crystallization, one of which is disordered in the lattice. Density measurements (Table I) confirmed that both  $\text{CH}_2\text{Cl}_2$  sites are fully occupied. The structure of the anion is presented in Figure 1. The  $\{\text{Fe}_4\text{O}_2\}^{8+}$  core has approximate  $C_2$  symmetry, in contrast to the slightly distorted (toward  $C_{2h}$ )  $D_{2h}$  symmetry displayed by the same core in  $[\text{Fe}_4\text{O}_2(\text{O}_2\text{CCF}_3)_8(\text{H}_2\text{O})_6]$  (**4**).<sup>15</sup> A comparison of these two structures is presented in Table IV. The  $\{\text{Fe}_4\text{O}_2\}^{8+}$  core of **4** is crystallographically required to be planar, whereas **1** has no imposed symmetry. The manner in which the idealized  $D_{2h}$  symmetry of **4** may be distorted

(23) (a) Gorun, S. M.; Lippard, S. J. *Nature (London)* **1986**, *319*, 666-668. (b) Gorun, S. M.; Papaefthymiou, G. C.; Frankel, R. B.; Lippard, S. J. *J. Am. Chem. Soc.* **1987**, *109*, 3337-3348.

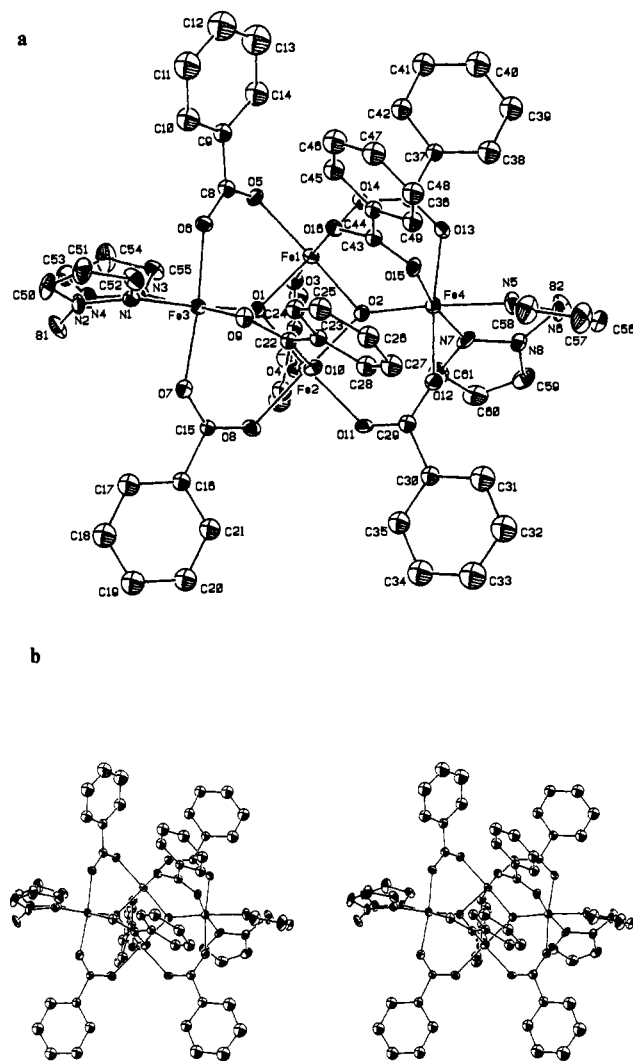


Figure 1. (a) ORTEP drawing of **1** (full view with atom labeling). (b) ORTEP drawing of **1** (stereoview).

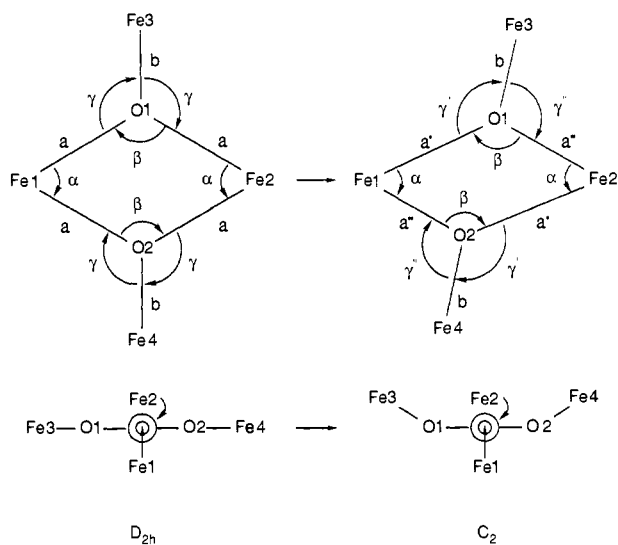


Figure 2. Two views of the distortions of the  $\{\text{Fe}_4\text{O}_2\}^{8+}$  core from  $D_{2h}$  to  $C_2$ .

toward the idealized  $C_2$  symmetry of **1** is illustrated in Figure 2. Selected distances and angles for the  $\{\text{Fe}_4\text{O}_2\}^{8+}$  core in **1** are shown in Figure 3; a more complete listing is given in Table III. In addition to the two  $\mu_3$ -oxo groups, there are seven bridging carboxylate ligands in the tetranuclear structure, one each between

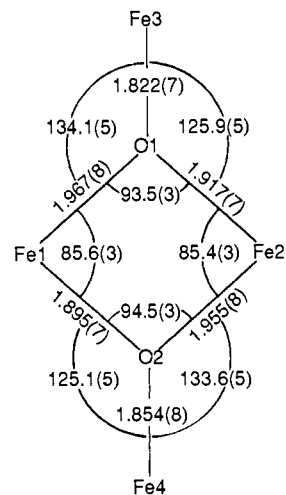


Figure 3. Bond distances (Å) and angles (deg) within the  $\{\text{Fe}_4\text{O}_2\}^{8+}$  core of **1**.

Table V

Least-Squares Planes in $[\text{Fe}_4\text{O}_2(\text{O}_2\text{CPh})_7(\text{H}_2\text{B}(\text{pz})_2)]^-$						
plane no.	atoms <sup>a</sup>	plane no.	atoms <sup>a</sup>	plane no.	atoms <sup>a</sup>	
1	Fe1Fe2O1O2	3	Fe1Fe2Fe3	5	Fe1Fe2Fe3O1	
2	Fe1Fe2Fe3Fe4	4	Fe1Fe2Fe4	6	Fe1Fe2Fe4O2	
Deviations from Plane (Å)						
atom	1	2	3	4	5	6
Fe1	0.065	0.473	0.000	0.000	-0.061	0.057
Fe2	0.064	0.465	0.000	0.000	-0.055	0.064
Fe3	-0.854	-0.469	0.000	1.787	-0.085	1.828
Fe4	-0.893	-0.469	-1.789	0.000	-1.826	0.085
O1	-0.064	0.332	0.270	0.531	0.201	0.582
O2	-0.065	0.348	-0.509	-0.278	-0.557	-0.207

<sup>a</sup> Used to define the plane.

iron atom pairs Fe1Fe2, Fe1Fe3, and Fe2Fe4 and two between Fe2Fe3 and Fe1Fe4. On the other hand, **4** has four identical bridging carboxylates, similar to two of the groups in **1**. The remaining carboxylates in **4** are terminally coordinated and monodentate.

It is likely that the planar structure of **4** is representative of the "preferred" geometry of the  $\{\text{Fe}_4\text{O}_2\}^{8+}$  core, while the decidedly nonplanar  $\{\text{Fe}_4\text{O}_2\}^{8+}$  unit of **1** is a consequence of the additional bridging carboxylate groups. Specifically, the iron atoms that are doubly bridged are apparently "pulled" closer to one another (Fe1...Fe4, 3.326 Å; Fe2...Fe3, 3.330 Å) than are those that are only singly bridged (Fe1...Fe3, 3.489 Å; Fe2...Fe4, 3.500 Å). In order to accommodate this situation, atoms Fe3 and Fe4 are displaced by 0.9 Å in the same direction from the mean plane of the  $\text{Fe}_2\text{O}_2$  inner core.

Deviations of atoms from several least-squares planes in the  $\{\text{Fe}_4\text{O}_2\}^{8+}$  core (Table V) further illustrate this point. Just as there are two long and two short Fe...Fe separations, there are also two long (Fe1-O1, Fe2-O2) and two short (Fe1-O2, Fe2-O1)  $\mu_3$ -oxo-iron bonds in the inner  $\text{Fe}_2\text{O}_2$  core. There is no evidence for a similar distortion in **4**. Each iron atom is in a distorted octahedral environment, with Fe1 having the largest range of idealized orthogonal (cis) angles (84.0–98.2°). Fe-N and Fe-O bond distances are typical of high-spin Fe(III) coordination complexes.<sup>4,24,25a-i</sup> The Fe-N distances for the pyrazole group trans to

(24) See for example: (a) Gorun, S. M.; Lippard, S. J. *J. Am. Chem. Soc.* **1985**, *107*, 4568–4570. (b) Murray, K. S. *Coord. Chem. Rev.* **1974**, *12*, 1–35. (c) Anderson, B. F.; Webb, J.; Buckingham, D. A.; Robertson, G. B. *J. Inorg. Biochem.* **1982**, *16*, 21–32. (d) Sinn, E.; Sim, G.; Dose, E. V.; Tweedle, M. F.; Wilson, L. J. *J. Am. Chem. Soc.* **1978**, *100*, 3375–3390. (e) Thich, J. A.; Toby, B. H.; Powers, D. A.; Potenza, J. A.; Schugar, H. *Inorg. Chem.* **1981**, *20*, 3314–3317.

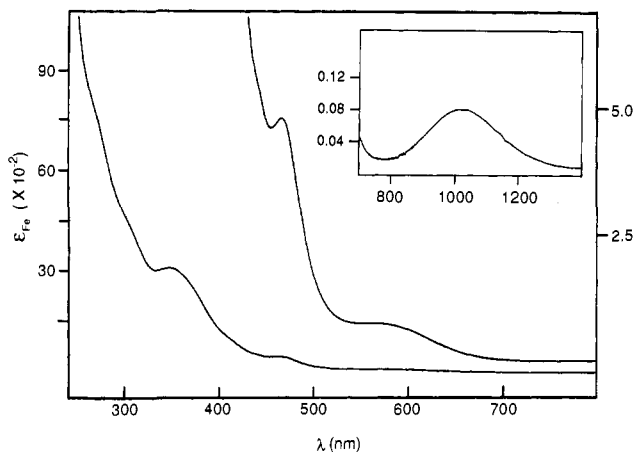


Figure 4. UV-vis/near-IR spectrum of **1** in 0.5 mM CH<sub>2</sub>Cl<sub>2</sub> solution.

Table VI. Comparison of the UV-vis/near-IR Spectra [ $\lambda$  ( $\epsilon$ )] of [Fe<sub>4</sub>O<sub>2</sub>(O<sub>2</sub>CPh)<sub>7</sub>(H<sub>2</sub>B(pz)<sub>2</sub>)<sub>2</sub>]<sup>-</sup> (**1**) and [Fe<sub>2</sub>O(O<sub>2</sub>CCH<sub>3</sub>)<sub>2</sub>(HB(pz)<sub>3</sub>)<sub>2</sub>]<sup>-</sup> (**5**)

<b>1</b> <sup>a</sup>	<b>5</b> <sup>b</sup>	<b>1</b> <sup>a</sup>	<b>5</b> <sup>b</sup>
350 (3300)	339 (4640)	565 (73)	695 (70)
	457 (505)	1020 (8)	995 (3.5)
467 (470)	492 (460)		

<sup>a</sup> Extinction coefficients are reported (cm<sup>-1</sup> M<sup>-1</sup>) per iron atom.  
<sup>b</sup> From ref 4b.

the short Fe-( $\mu_3$ -O) bonds are marginally longer than those cis to it, an effect that is much less dramatic than in [Fe<sub>2</sub>O(O<sub>2</sub>CCH<sub>3</sub>)<sub>2</sub>(HB(pz)<sub>3</sub>)<sub>2</sub>]<sup>-</sup>.<sup>4</sup> The shortest Fe-( $\mu_3$ -O) lengths (Fe3-O1, 1.822 (7) Å; Fe4-O2, 1.854 (8) Å) are longer than the high end of the range of distances typically observed for Fe-O-Fe complexes (~1.73–1.82 Å)<sup>25</sup> but are substantially shorter than those observed for typical Fe<sub>3</sub>( $\mu_3$ -O) species (1.9 Å).<sup>26</sup> The average Fe-( $\mu_3$ -O) bond distance of 1.90 Å in **1**, however, is very close to the latter value.

Tetranuclear M<sub>4</sub>O<sub>2</sub> species similar to **1** have been observed in other compounds. In tin chemistry, the structures of [Sn<sub>4</sub>(OC<sub>4</sub>H<sub>8</sub>)<sub>2</sub>( $\mu_3$ -O)<sub>2</sub>(*o*-NO<sub>2</sub>C<sub>6</sub>H<sub>4</sub>COO)<sub>8</sub>]<sup>27</sup> and [Me<sub>4</sub>Sn<sub>2</sub>Cl<sub>2</sub>O]<sub>2</sub><sup>28</sup> are known. The inner {Fe<sub>4</sub>O<sub>2</sub>}<sup>8+</sup> core of [Fe<sub>8</sub>O<sub>2</sub>(OH)<sub>12</sub>(TACN)<sub>6</sub>]<sup>8+</sup> bears a marked resemblance to the {Fe<sub>4</sub>O<sub>2</sub>}<sup>8+</sup> geometry described here. Recently, the compounds [Mn<sub>4</sub>O<sub>2</sub>(O<sub>2</sub>CCH<sub>3</sub>)<sub>7</sub>(bipy)<sub>2</sub>]<sup>+</sup> and [Mn<sub>4</sub>O<sub>2</sub>(O<sub>2</sub>CC<sub>6</sub>H<sub>5</sub>)<sub>7</sub>(bipy)<sub>2</sub>] have been reported.<sup>29</sup> The Mn<sub>4</sub>O<sub>2</sub> core described for these Mn(III) and mixed valence Mn(III)/Mn(IV) complexes is analogous to the one in **1** and **2**.<sup>29</sup> The [M<sub>4</sub>O<sub>2</sub>(O<sub>2</sub>CR)<sub>7</sub>L<sub>2</sub>] stoichiometry may turn out to be a common one for a number of metal ions.

(25) (a) Lippard, S. J.; Schugar, H.; Walling, C. *Inorg. Chem.* **1967**, *6*, 1825–1831. (b) Fleischer, E.; Hawkinson, S. *J. Am. Chem. Soc.* **1967**, *89*, 720–721. (c) Hoffman, A. B.; Collins, D. M.; Day, V. W.; Fleischer, E. B.; Srivastava, T. S.; Hoard, J. L. *J. Am. Chem. Soc.* **1972**, *94*, 3620–3626. (d) Gerloch, M.; McKenzie, E. D.; Towl, A. D. C. *J. Chem. Soc. A* **1969**, 2850–2858. (e) Gözen, S.; Peters, R.; Owston, P. G.; Tasker, P. A. *J. Chem. Soc., Chem. Commun.* **1980**, 1191–1201. (f) Coggon, P.; McPhail, A. T.; Mabbs, F. E.; McLachlan, V. N. *J. Chem. Soc. A* **1971**, 1014–1019. (g) Atovmyan, L. O.; D'yachenko, O. A.; Soboleva, S. V. *J. Struct. Chem.* **1970**, *11*, 517–518. (h) Davies, J. E.; Gatehouse, B. M. *Cryst. Struct. Commun.* **1972**, *1*, 115–120. (i) Welss, M. C.; Goedken, V. L. *Inorg. Chem.* **1979**, *18*, 819–826. (j) Drew, M. G. B.; McKee, V.; Nelson, S. M. *J. Chem. Soc., Dalton Trans.* **1978**, 80–84. (k) Schmidbauer, H.; Zybilla, C. E.; Neugebauer, D. *Angew. Chem., Int. Ed. Engl.* **1983**, *22*, 156 and 161. (l) Dehnlücke, K.; Prinz, H.; Massa, M.; Pebler, J.; Schmidt, R. Z. *Z. Anorg. Allg. Chem.* **1983**, *499*, 20–30. (m) Reiff, W. M.; Witten, E. H.; Mottle, K.; Garafalo, A. R. *Inorg. Chim. Acta* **1983**, *77*, L83–L88.

(26) (a) Thundathil, R. V.; Holt, E. M.; Holt, S. L.; Watson, K. J. *J. Am. Chem. Soc.* **1977**, *99*, 1818–1823. (b) Anzenhofer, K.; DeBoer, J. J. *Recl. Trav. Chim. Pays-Bas* **1969**, *88*, 286–288.

(27) Ewings, P. F. R.; Harrison, P. G.; Morris, A.; King, T. J. *J. Chem. Soc., Dalton Trans.* **1976**, 1602.

(28) Dakternieks, D.; Gable, R. W.; Hoskins, B. F. *Inorg. Chim. Acta* **1984**, *85*, L43–L44.

(29) Vincent, J. B.; Christmas, C.; Huffman, J. C.; Christou, G.; Chang, H.-R.; Hendrickson, D. N. *J. Chem. Soc., Chem. Commun.* **1987**, 236–238.

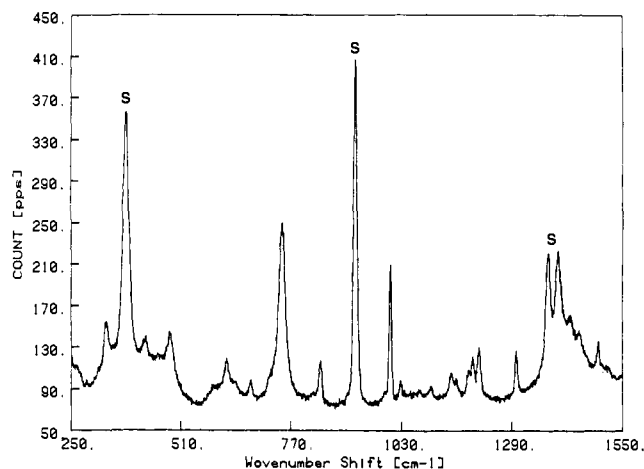


Figure 5. Raman spectrum of **1** in CH<sub>3</sub>CN solution with 488-nm excitation. The peaks marked S are from the solvent, except for the feature at 1398 cm<sup>-1</sup>.

Table VII. Selected Data from Magnetic Measurements for (Et<sub>4</sub>N)[Fe<sub>4</sub>O<sub>2</sub>(O<sub>2</sub>CPh)<sub>7</sub>(H<sub>2</sub>B(pz)<sub>2</sub>)<sub>2</sub>] (**1**)<sup>a</sup>

T, K	10 <sup>3</sup> χ <sub>M</sub>	μ <sub>Fe</sub>	T, K	10 <sup>3</sup> χ <sub>M</sub>	μ <sub>Fe</sub>
6.0	2.186	0.162	130.3	7.712	1.42
15.0	1.387	0.204	150.6	7.921	1.55
30.0	2.942	0.420	180.6	8.180	1.72
50.0	5.423	0.737	211.0	8.423	1.89
70.0	6.507	0.955	250.3	8.705	2.09
90.1	7.081	1.13	290.2	8.959	2.28
110.2	7.449	1.28	300.2	9.013	2.33

<sup>a</sup> χ<sub>M</sub> is the molar susceptibility corrected for underlying diamagnetism, and μ<sub>Fe</sub>, the magnetic moment calculated as 1/2(2.829)(χ<sub>M</sub>T)<sup>1/2</sup> per iron. Complete data are available in Table S5.

**Spectroscopic, Magnetic, and Mössbauer Properties.** The UV-vis/near-IR spectrum of **1** in CH<sub>2</sub>Cl<sub>2</sub> solution is displayed in Figure 4. It consists principally of four maxima at 350, 467, 565, and 1020 nm. This optical spectrum appears to be characteristic of the {Fe<sub>4</sub>O<sub>2</sub>}<sup>8+</sup>, or perhaps the {Fe<sub>4</sub>O<sub>2</sub>(O<sub>2</sub>CR)<sub>4</sub>}<sup>4+</sup>, core since very similar features are also observed for [Fe<sub>4</sub>O<sub>2</sub>(O<sub>2</sub>CPh)<sub>4</sub>(BICO)<sub>2</sub>(BICOH)<sub>2</sub>]<sup>2+</sup>.<sup>11</sup> Unfortunately, spectral data are not available for [Fe<sub>4</sub>O<sub>2</sub>(O<sub>2</sub>CCF<sub>3</sub>)<sub>8</sub>(H<sub>2</sub>O)<sub>6</sub>]. As illustrated in Table VI, there is a distinct similarity between the spectrum of **1** and that of [Fe<sub>2</sub>O(O<sub>2</sub>CCH<sub>3</sub>)<sub>2</sub>(HB(pz)<sub>3</sub>)<sub>2</sub>]<sup>-</sup> (**5**).<sup>4</sup> In terms of band position and intensity, there is almost a one-to-one correspondence between the optical spectra of the two compounds. The lowest energy absorption band in **1**, considered to arise from the <sup>6</sup>A<sub>1</sub> → <sup>4</sup>T<sub>1</sub> (<sup>4</sup>G) d-d transition, is shifted by 25 nm from its position in the spectrum of **5**. The next highest energy transition (565 nm), presumably responsible for the green color of **1**, would be the <sup>6</sup>A<sub>1</sub> → <sup>4</sup>T<sub>2</sub> (<sup>4</sup>G) band, by analogy to **5**. As is the case for **5**, this absorption is unusually intense for a high-spin Fe(III) d-d transition and may be enhanced as a result of the lowered symmetry around iron or perhaps by spin-spin interactions between metal ions. Although the exact nature of the bands at 467 and 350 nm cannot be assigned with the available data, they do have counterparts in the spectrum of **5** and are thought to be principally charge transfer in origin.

A resonance Raman spectrum of **1** in CH<sub>3</sub>CN solution is presented in Figure 5. Using 488-nm excitation, one observes principally a single resonance-enhanced band. This band falls at 746 cm<sup>-1</sup>, very close to the position (751 cm<sup>-1</sup>) of the asymmetric Fe-O-Fe stretch in the IR spectrum of **5**. This peak is clearly the most prominent absorption associated with the {Fe<sub>4</sub>O<sub>2</sub>}<sup>8+</sup> core in the spectrum. Several other metal-oxo species absorb in the region 600–750 cm<sup>-1</sup>, owing to their oxo-bridged core structures. For example, a band at 688 cm<sup>-1</sup> in the IR spectrum of [Mn<sub>2</sub>O<sub>2</sub>(bipy)<sub>4</sub>]<sup>3+</sup>,<sup>30</sup> the Mn<sub>2</sub>O<sub>2</sub> core of which<sup>31</sup> is reminiscent of

(30) Cooper, S. R.; Calvin, M. *J. Am. Chem. Soc.* **1977**, *99*, 6623–6630.

(31) Plaskin, P. M.; Stouffer, R. C.; Mathew, M.; Palenik, G. J. *J. Am. Chem. Soc.* **1972**, *94*, 2121–2122.

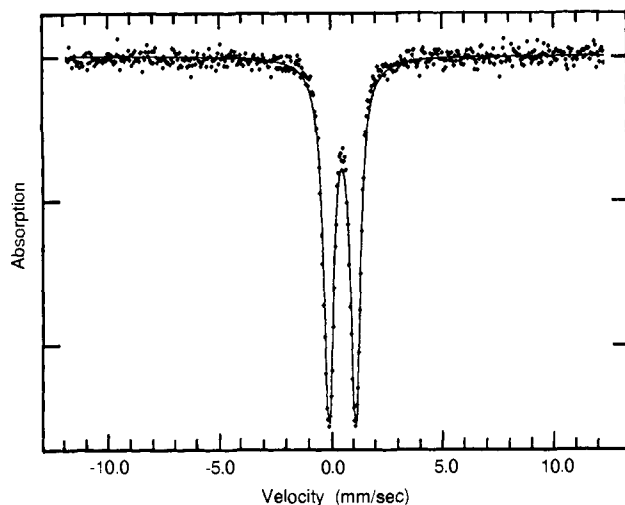


Figure 6. Mössbauer spectrum of **1** at 4.2 K (zero applied field).

Table VIII. Mössbauer Data for  $(Et_4N)[Fe_4O_2(O_2CPh)_7(H_2B(pz)_2)_2] (1)$

T, K	$\delta$ , <sup>a</sup> mm/s	$\Delta E_Q$ , mm/s	T, K	$\delta$ , <sup>a</sup> mm/s	$\Delta E_Q$ , mm/s
4.2	0.53	1.21	230	0.45	1.20
80	0.52	1.21	295	0.41	1.19

<sup>a</sup>  $\delta$  is relative to metallic iron at room temperature.

the inner  $Fe_2O_2$  core of **1**, has been assigned to a vibrational mode associated with the oxo-bridged dimanganese moiety on the basis of  $^{18}O$ -substitution studies.<sup>30</sup> The trinuclear iron(III) carboxylate cation  $[Fe_3O(O_2CCH_3)_6(H_2O)_3]^+$  displays an asymmetric  $M_3O$ -type stretch at  $609\text{ cm}^{-1}$ .<sup>32</sup> Although it has a distinctly different structure,  $[Mn_4O_6(TACN)_4]^{4+}$ , which has an adamantane-like  $Mn_4O_6$  core,<sup>33</sup> has a prominent band in the IR spectrum at  $730\text{ cm}^{-1}$  that is apparently characteristic of the  $\{Mn_4O_6\}^{4+}$  aggregate.

Magnetic measurements were made on a solid sample of **1** over the temperature range 6–300 K. An abbreviated set of results is shown in Table VII, the full set being provided in Table S5 (supplementary material). The room-temperature magnetic moment per iron atom ( $\mu_{Fe}(300\text{ K}) = 2.33\ \mu_B$ ) is indicative of strong antiferromagnetic interactions within the  $\{Fe_4O_2\}^{8+}$  cluster. The coupling is weaker, however, than in oxo-bridged binuclear complexes (**5**,  $\mu_{Fe}(300\text{ K}) = 1.71\ \mu_B$ ), owing to the substantially longer Fe–oxo distances in **1**. The distorted tetrahedral  $Fe_4$  complex,  $[Fe_4L_2O_2(OH)_2]^{4-}$  ( $L = N,N'$ -(2-hydroxy-5-methyl-1,3-xylylene)bis[*N*-(carboxymethyl)glycine]), displays a lower effective moment ( $1.71\ \mu_B$ )<sup>13</sup> than **1**, presumably owing to its markedly shorter Fe–O–Fe bond lengths (1.790, 1.792 Å), which more effectively mediate the magnetic exchange between iron atoms. On the other hand, another tetranuclear complex recently discovered<sup>14</sup> has Fe–oxo bond lengths (1.828 (4), 1.830 (4) Å) more similar to those in **1** and a reported magnetic moment of  $2.49\ \mu_B$  per iron at 260 K. The magnetic moment of **1** decreases with decreasing temperature to a value of  $0.16\ \mu_B$  at 6.0 K. The susceptibility reaches a minimum at 15 K and starts to increase between 15 and 6 K, probably due to the presence of a paramagnetic impurity. Except for this slight rise in moment at the lowest temperatures, the temperature-dependent behavior of the susceptibility of **1** would appear to be consistent with an  $S = 0$  electronic ground state. Preliminary attempts to fit the susceptibility versus temperature data to simple spin–exchange coupling models indicated the need for more extensive theoretical analysis, currently being undertaken.

The Mössbauer spectrum of **1** at 4.2 K is displayed in Figure 6. The isomer shifts and quadrupole splitting values at four temperatures in zero applied magnetic field are listed in Table

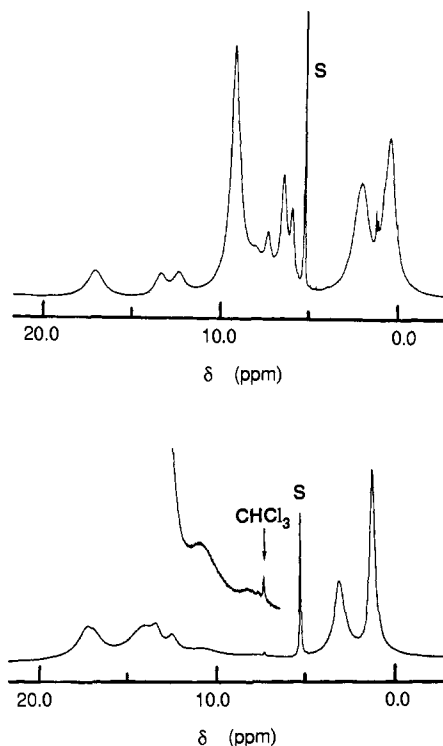


Figure 7. Proton NMR spectra of **1** (top) and **2** (bottom) in  $CD_2Cl_2$  solution. The peaks marked S are from the solvent.

VIII. The isomer shift of 0.53 mm/s (relative to metallic iron at room temperature) at 4.2 K is typical for high-spin ferric complexes. For example,  $[Fe_2O(O_2CCH_3)_2(HB(pz)_2)_2]$  has an isomer shift of 0.52 mm/s at 4.2 K. The  $\delta$  value for **4** was reported to be 0.81 mm/s at 80 K, however.<sup>16</sup> The reference point for this measurement was not given. The spectra of **1** were fit with a single quadrupole doublet between 4.2 and 295 K, despite the inequivalence of Fe and Fe' sites (Table IV) in the solid-state structure. The  $\Delta E_Q$  value of 1.21 mm/s at 4.2 K is consistent with a substantial distortion from octahedral symmetry. Quadrupole splittings for oxo-bridged binuclear complexes generally fall in the range 1.5–2.0 mm/s.<sup>4b</sup> The distortion from octahedral symmetry is greater in these compounds, since the  $\mu$ -oxo distances are shorter ( $\sim 1.71$ – $1.8\ \text{\AA}$ ) than the shortest Fe– $O_{oxo}$  bond in **1**, and thus the  $\Delta E_Q$  values tend to be greater. In contrast, the Mössbauer spectrum of **4** displays a partially resolved pair of doublets at 300 K and a well-resolved pair at 80 K. The Fe'/Fe site inequivalence in **4** is clearly enhanced with respect to **1**. One possible explanation for this difference is apparent from inspection of Table IV, assuming the simple rule that the principal distortion is due to the length of the Fe–( $\mu_3$ -oxo) bond and that this distortion from octahedral symmetry is in turn responsible for a greater  $\Delta E_Q$  value. The Fe– $O_{oxo}$  bonds in **4** divide into two very distinct sets, with the closest approach between the two sets being 0.094 Å. For **1**, however, the Fe'–O and Fe–O distances form a more continuous set, with the closest approach being 0.041 Å. Thus, Fe and Fe' are not as structurally distinct in **1** as they are in **4**, which accounts for the inability to resolve two pairs of quadrupole doublets.

**Solution NMR Structural Studies.** The proton NMR spectra of **1** and **2** (Figure 7) suggest that their basic tetranuclear structures are retained in solution. While the spectra are not as informative as for the binuclear complexes,<sup>4</sup> some analysis is possible. The resonances are concentration dependent with some line widths increasing with increasing concentrations, probably due to ion pairing. As expected for such a case, switching from  $CD_2Cl_2$  to a more polar solvent,  $CD_3CN$ , changes the appearance of the spectra.

The resonances occurring farthest downfield in the spectrum of **1** dissolved in  $CD_2Cl_2$  can be assigned to 8 of the 12 pyrazolyl ring protons. Integration of these signals reveals that the resonance

(32) Johnson, M. K.; Powell, D. B.; Cannon, R. D. *Spectrochim. Acta, Part A* **1981**, *37A*, 995–1006.

(33) Wieghardt, K.; Bossek, U.; Gebert, W. *Angew. Chem., Int. Ed. Engl.* **1983**, *22*, 328–329.

at 17.1 ppm and the pair at 13.5 and 12.5 ppm each correspond to 4 protons. Although it is impossible definitively to assign these resonances without further experiments, they most likely arise from pyrazolyl H4 and H5 protons since, in the analogous binuclear compound **5**, the H3 proton resonance is broad and occurs farther upfield in the spectrum. Although there are two symmetrically inequivalent sets of pyrazole rings in **1**, the resonances for either the H4 or the H5 protons must be coincident, forming the peak at 17.1 ppm, while the other set of protons gives rise to the pair of peaks at 13.5 and 12.5 ppm. Similarly, in the spectrum of **2**, signals are observed at 17.3, 13.5, and 12.4 ppm, but they are overlapped by two broader signals at 16.9 and 14.2 ppm (Figure 7). The spectrum of **2** in CD<sub>2</sub>Cl<sub>2</sub> exhibits two additional broad resonances at 10.9 and 8.0 ppm. Either of these latter two bands could arise from the pyrazole ring H3 proton; the remaining three of this set of four resonances arise from methyl groups of the bridging acetates. In CD<sub>3</sub>CN, the pyrazole ring resonances appear sharper but are still overlapped by the methyl resonances. Also, the broad band at 8.1 ppm appears much sharper and occurs at 7.7 ppm, and an additional small resonance is apparent at 6.6 ppm.

The H3 pyrazole ring resonances cannot be observed in the spectrum of **1**, owing to the occurrence of numerous broad bands between 5 and 11 ppm arising from phenyl ring protons of the bridging benzoates. Three relatively sharp peaks at 7.3, 6.5, and 6.0 ppm are probably due to the para protons, which are farthest from the paramagnetic iron centers. From the ratio of intensities it appears that the para protons of two of the symmetrically distinct benzoates must be accidentally coincident at 6.5 ppm. When the spectrum is recorded in CD<sub>3</sub>CN, a shoulder is visible on the peak at 6.5 ppm.

The very broad signals at 2.1 and 0.6 ppm in the spectrum of **1** dissolved in CD<sub>2</sub>Cl<sub>2</sub> are those most dramatically affected by a change in solvent. In CD<sub>3</sub>CN, these peaks appear with line widths only one-fourth of the values seen in CD<sub>2</sub>Cl<sub>2</sub> and at chemical shift values of 2.9 and 1.0 ppm. These resonances, the first of which lies on top of the broad B-H resonances of the H<sub>2</sub>B(pz)<sub>2</sub><sup>-</sup> ligands, are assigned to the methylene and methyl protons, respectively, of the Et<sub>4</sub>N<sup>+</sup> cation. The effects on the analogous peaks at 3.1 and 1.2 ppm in the spectrum of **2** are similar but less dramatic. These two peaks become sharper, but no significant change in chemical shift is observed.

The room-temperature magnetic susceptibility of **1** in solution was measured by the Evans method.<sup>22</sup> A value for μ<sub>Fe</sub> of 2.34 μ<sub>B</sub> at 295 K calculated by this method is in close agreement with the solid-state value of 2.33 μ<sub>B</sub> at 300 K. A value of 2.41 μ<sub>B</sub> was measured for **2**. The results are consistent with retention of the tetranuclear [Fe<sub>4</sub>O<sub>2</sub>]<sup>8+</sup> core in solution, especially with respect to dissociation into {Fe<sub>2</sub>O}<sup>4+</sup> units. The larger magnetic moment of the tetranuclear compared to dinuclear complexes is reflected in the magnitude of the isotropic shifts observed for pyrazolyl protons.

The most shifted resonance is found at 17.1 ppm in **1**, compared with 12.2 ppm in **5**.<sup>4b</sup>

### Conclusions

Conceptually, the residual donating capacity of a μ-oxo atom in the {Fe<sub>2</sub>O}<sup>4+</sup> core results in dimerization to form {Fe<sub>4</sub>O<sub>2</sub>]<sup>8+</sup>. This reaction pathway is not available to the {Fe<sub>2</sub>O}<sup>4+</sup> core in heme-rhithrin, since it is sterically protected by the polypeptide chain. From the present study, it appears that steric hindrance may be required in order to obtain functional models for Hr and RR, as was the case for hemoglobin models.<sup>34</sup> The tetranuclear complex obtained from the present work was characterized by crystallographic, spectroscopic, Mössbauer, and preliminary magnetic measurements. Distortions from the planarity manifest in a similar compound, [Fe<sub>4</sub>O<sub>2</sub>(O<sub>2</sub>CCF<sub>3</sub>)<sub>8</sub>(H<sub>2</sub>O)<sub>6</sub>], presumably are caused by strain induced by additional bridging carboxylate groups in **1**. Paramagnetically shifted NMR spectra and solution magnetic susceptibility results provide strong evidence that the tetranuclear structure of [Fe<sub>4</sub>O<sub>2</sub>(O<sub>2</sub>CR)<sub>7</sub>(H<sub>2</sub>B(pz)<sub>2</sub>)<sub>2</sub>]<sup>-</sup>, where R = Ph or Me, persists in solution.

**Acknowledgment.** This work was supported by National Institutes of Health (NIH) Research Grant GM32134 from the National Institute of General Medical Sciences. M.E.R. was a National Science Foundation Predoctoral Fellow, and W.H.A. gratefully acknowledges support under NCI Training Grant CA09112. Raman spectra were obtained at the MIT Regional Laser Center, which is a National Service Foundation Regional Instrumentation Facility. We thank G. Papaefthymiou and R. B. Frankel of the Francis Bitter National Magnet Laboratory for Mössbauer spectra, K. Suryanarayan for preparing ORTEP diagrams, and H. J. Schugar for providing us with a preprint of ref 14.

**Supplementary Material Available:** Tables of non-hydrogen atom thermal parameters, hydrogen atom positional and thermal parameters, ligand, cation, and solvent molecular geometry, and magnetic susceptibility data (Tables S2-S5) (11 pages); table of observed and calculated structure factor amplitudes (Table S1) (23 pages). Ordering information is given on any current masthead page.

(34) (a) Collman, J. P.; Brauman, J. I.; Iverson, B. L.; Sessler, J. L.; Morris, R. M.; Gibson, Q. H. *J. Am. Chem. Soc.* **1983**, *105*, 3052-3064. (b) Traylor, T. G.; Koga, N.; Deardurff, L. A.; Swepston, P. N.; Ibers, J. A. *Ibid.* **1984**, *106*, 5132-5143. (c) Ward, B.; Wang, C.-B.; Chang, C. K. *Ibid.* **1981**, *103*, 5236-5238. (d) Busch, D. H.; Zimmer, L. L.; Grzybowski, J. J.; Olszanski, D. J.; Jackels, S. C.; Callahan, R. C.; Christoph, G. G. *Proc. Natl. Acad. Sci. U.S.A.* **1981**, *78*, 5919-5923. (e) Hashimoto, T.; Dyer, R. L.; Crossley, M. J.; Baldwin, J. E.; Basolo, F. *J. Am. Chem. Soc.* **1982**, *104*, 2101-2109. (f) Battersby, A. R.; Hamilton, A. D. *J. Chem. Soc., Chem. Commun.* **1980**, 117-119.

## Raney Nickel Reductions of Chlorophyll Derivatives: Hydroporphyrins in the Anhydro Series

Kevin M. Smith\* and Daniel J. Simpson

Contribution from the Department of Chemistry, University of California, Davis, California 95616. Received February 23, 1987

**Abstract:** Raney nickel reductions of nickel(II) anhydromesorhodoporphyrin XV (**17**) provide a series of readily separable nickel(II) hydroporphyrins. Apart from the two expected isobacteriochlorins **19** and **22**, two hexahydroporphyrins **20** and **21** were obtained as the major reduction product (32%). Hexahydroporphyrins of the pyrrocorphin type (**7**) observed in Raney nickel reductions of pheophorbides were not observed. The most novel hydroporphyrin isolated was an octahydroporphyrin **23** obtained in 5% yield by further reduction of the hexahydroporphyrin isomers.

There are a variety of porphyrinoid macrocycles in which the chromophore is in some reduced state. The most common of

these, the dihydroporphyrins (chlorins), are generally associated with magnesium-containing photosynthetic pigments. However,